Blood pressure, executive function, and network connectivity in middle-aged adults at risk of dementia in late life

Lisanne M. Jenkins[a,1] , Alexandr Kogan[a], Matthew Malinab[b], Carson Ingo[c,d], Sanaz Sedaghat[c,e], Nick R. Bryan[f], Kristine Yaffe[g], Todd B. Parrish[d,h,i], Alexander J. Nemeth[c,h] , Donald M. Lloyd-Jones[e,j,k] , Lenore J. Launer[l] , Lei Wang[a,h] , and Farzaneh Sorond[c]

[a]Department of Psychiatry and Behavioral Sciences, Feinberg School of Medicine, Northwestern University, Chicago, IL 60611; [b]Faculty of Applied Sciences, Simon Fraser University, Burnaby, BC, Canada, V5A 1S6; [c]Department of Neurology, Feinberg School of Medicine, Northwestern University, Chicago, IL 60611; [d]Department of Physical Therapy and Human Movement Sciences, Feinberg School of Medicine, Northwestern University, Chicago, IL 60611; [e]Department of Preventive Medicine, Feinberg School of Medicine, Northwestern University, Chicago, IL 60611; [f]Department of Radiology, University of Pennsylvania School of Medicine, Philadelphia, PA 19103; [g]Weill Institute for Neurosciences, University of California, San Francisco, CA 94121; [h]Department of Radiology, Feinberg School of Medicine, Northwestern University, Chicago, IL 60611; [i]McCormick School of Engineering, Northwestern University, Chicago, IL 60208; [j]Department of Medicine, Feinberg School of Medicine, Northwestern University, Chicago, IL 60611; [k]Department of Pediatrics, Feinberg School of Medicine, Northwestern University, Chicago, IL 60611; and [l]Intramural Research Program, National Institute on Aging, Baltimore, MD 20814

Midlife blood pressure is associated with structural brain changes, cognitive decline, and dementia in late life. However, the relationship between early adulthood blood pressure exposure, brain structure and function, and cognitive performance in midlife is not known. A better understanding of these relationships in the preclinical stage may advance our mechanistic understanding of vascular contributions to late-life cognitive decline and dementia and may provide early therapeutic targets. To identify resting-state functional connectivity of executive control networks (ECNs), a group independent components analysis was performed of functional MRI scans of 600 individuals from the Coronary Artery Risk Development in Young Adults longitudinal cohort study, with cumulative systolic blood pressure (cSBP) measured at nine visits over the preceding 30 y. Dual regression analysis investigated performance-related connectivity of ECNs in 578 individuals (mean age 55.5 ± 3.6 y, 323 female, 243 Black) with data from the Stroop color–word task of executive function. Greater connectivity of a left ECN to the bilateral anterior gyrus rectus, right posterior orbitofrontal cortex, and nucleus accumbens was associated with better executive control performance on the Stroop. Mediation analyses showed that while the relationship between cSBP and Stroop performance was mediated by white matter hyperintensities (WMH), resting-state connectivity of the ECN mediated the relationship between WMH and executive function. Increased connectivity of the left ECN to regions involved in reward processing appears to compensate for the deleterious effects of WMH on executive function in individuals across the burden of cumulative systolic blood pressure exposure in midlife.

fMRI | resting-state connectivity | executive function | white matter hyperintensities | systolic blood pressure

Vascular risk factors (VRF) such as hypertension in midlife are associated with cognitive decline in late life (1–4). Notably, deficits in executive function, such as cognitive flexibility or inhibitory control, are early and "prominent" in vascular-related neurocognitive disorders (5). VRF are also associated with structural MRI brain changes such as white matter hyperintensities (WMH) (6), gray matter atrophy (7), and subcortical morphological changes (8), which may not be reversible. However, functional MRI (fMRI) changes may be detectable prior to irreversible structural damage. fMRI studies have shown that VRF are associated with reduced functional connectivity of brain networks and that this reduced network connectivity is associated with cognitive decline (9, 10). Understanding these relationships in midlife individuals and prior to the clinical onset of cognitive decline could

provide significant insight into imaging markers that may identify individuals at risk of cognitive impairment and mechanisms for targeted interventions.

In this study, we examined the relationship between blood pressure (BP), executive performance, and resting-state fMRI (rsfMRI) connectivity in participants from the brain substudy of the Coronary Artery Disease in Young Adults (CARDIA) longitudinal cohort study. We hypothesized that greater rsfMRI connectivity of executive control networks (ECN) would be related to better performance in an out-of-scanner executive control (Stroop) task. We further hypothesized that while the previously established relationship of systolic BP (SBP) to Stroop performance (11) would be mediated by WMH, the established relationship between WMH and executive function (12, 13) would be mediated by ECN connectivity.

Significance

The contribution of midlife vascular risk factors to brain structure and cognition in late life is well established. In this large cohort of midlife individuals, we replicated and extended previous findings of relationships between functional brain network connectivity and executive function in the context of white matter hyperintensities (WMH) and extended them to our measure of cumulative blood pressure exposure over 30 y from young adulthood. We report mediation of the relationship between WMH and executive function via functional connectivity. Our results support conclusions that neuroplastic reorganization of network connectivity may follow disruption to white matter tracks and furthermore suggest that this reorganization occurs early in the preclinical stage, prior to the onset of overt disease.

Materials and Methods

Participants. Participants were recruited from the brain imaging substudy of CARDIA. CARDIA is a longitudinal cohort study of VRF, which began in 1985 and recruited 5,115 individuals aged 18 to 30 y. At 30 y (Y_{30}) after baseline, a subset of 758 participants completed an MRI session at one of four sites (Chicago, Birmingham, Minnesota, and Oakland). Following quality control of rsfMRI (detailed in *MRI quality control* section) and excluding participants without Stroop data at Y_{30}, the final sample was 578. Demographic and VRF data are summarized in Table 1 and reported separately by site in *SI Appendix*, Table S1. Exclusion criteria were MRI contraindications, including body size too large for MRI bore and suspected pregnancy. Institutional review boards (IRBs) at each field center (Northwestern University IRB, The University of Alabama Birmingham IRB, the University of Minnesota IRB, and Kaiser Permanente Northern California IRB) and the coordinating center (University of Pennsylvania IRB) approved the CARDIA study annually. Written informed consent was provided at each examination for all participants.

Measures and Procedures.

BP. Among VRF, we focused on BP, given its robust association with WMH. Measurement of BP has been described previously (14, 15). BP was measured from the right arm brachial artery while the participant was seated. To investigate the cumulative burden of high BP and obtain an accurate measure of vascular burden, we used cumulative BP instead of a single BP measure. Cumulative systolic BP (cSBP) was calculated per previous CARDIA studies (14, 15) detailed in Fig. 1. For Y_0 to Y_{15}, a Hawksley random-zero sphygmomanometer was used, and for subsequent visits, an automated oscillometric BP monitor (Omron HEM-907XL) was used. A calibration study standardized values to the sphygmomanometer to eliminate machine bias (refer to ref. 14). Mean SBP (and mean diastolic BP [DBP]) was calculated between two consecutive visits, multiplied by the number of years between those two visits, and then summed to determine cSBP (and cDBP) over 30 y. cSBP and cDBP were normally distributed. All 578 participants had BP measures for Y_0 and Y_{30}, and all had BP measures for at least five separate visits. For Y_2, Y_5, Y_7, Y_{10}, Y_{15}, Y_{20}, and Y_{25}, BP data were unavailable for 18, 22, 26, 32, 32, 29, and 16 participants, respectively. In these instances, mean BP between two consecutive visits was calculated and the number of years between visits that this mean was multiplied by was adjusted as appropriate (Fig. 1).

Stroop color–word test. This executive function task requires individuals to respond to one stimulus dimension (ink color) while suppressing responses to another more prepotent dimension (word reading). Individuals are presented with words (names of colors) on a page that are printed in the same colored
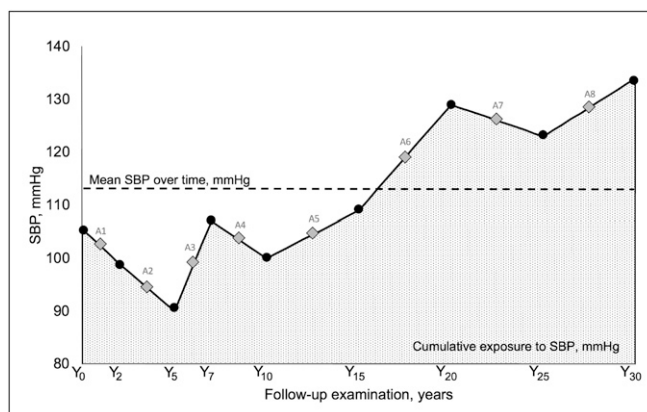

Fig. 1. Mean SBP (and mean DBP) was calculated between two consecutive visits, multiplied by the number of years between those two visits, and then summed to determine cSBP (and cDBP) over 30 y. This figure is an example of cSBP calculation across nine visits in one participant. Average SBP between consecutive visits is shown as A1 through A8. cSBP (mm Hg × years) was calculated as (A1 × 2 y + A2 × 3 y + A3 × 2 y + A4 × 3 y + A5 × 5 y + A6 × 5 y + A7 × 5 y + A8 × 5 y), shown by the shaded area. Note that not all participants completed all visits (see BP section of *Measures and Procedures*), so we report here the frequencies of duration (years) between consecutive visits: 2 y (i.e., Y_0–Y_2 and Y_5–Y_7) = 1,097; 3 y (Y_2–Y_5 and Y_7–Y_{10}) = 1,070; 5 y (Y_0–Y_5, Y_2–Y_7, Y_5–Y_{10}, Y_{10}–Y_{15}, Y_{15}–Y_{20}, Y_{20}–Y_{25} and Y_{25}–Y_{30}) = 2,348; 7 y (Y_0–Y_7) = 1; 8 y (Y_2–Y_{10} and Y_7–Y_{15}) = 16; 10 y (Y_0–Y_{10}, Y_5–Y_{15}, Y_{10}–Y_{20}, Y_{15}–Y_{25} and Y_{20}–Y_{30}) = 36; 13 y (Y_2–Y_{15} and Y_7–Y_{20}) = 7; 15 y (Y_5–Y_{20}, Y_{10}–Y_{25} and Y_{15}–Y_{30}) = 9; 18 y (Y_2–Y_{20} and Y_7–Y_{25}) = 3; 20 y (Y_5–Y_{25} and Y_{10}–Y_{30}) = 5; 23 y (Y_7–Y_{30}) = 2. Adapted from Yano et al. (14, 15).

ink (congruent trials) or a different color ink (incongruent trials). Reaction time and number of errors are recorded. An interference score is calculated by subtracting the score (time in seconds plus number of errors) on the incongruent trial from the score in the congruent trial. Higher scores indicate worse performance.

Category fluency test. This measure of semantic fluency (CatFluency) is a commonly used test of executive function (16). Participants are asked to name as many animals as they can in 60 s. The total score is calculated as the total number of correct, unique animals named within the time limit.

Montreal Cognitive Assessment. The Montreal Cognitive Assessment (MoCA) is a brief (10-min) screening tool for mild cognitive impairment (17). With a maximum score of 30, this instrument measures multiple cognitive abilities including short-term memory, visuospatial ability, multiple aspects of executive function (including cognitive flexibility, phonemic fluency, and verbal abstraction), attention, concentration, working memory, and language.

Digit-symbol substitution test. This pencil and paper test requires sequential matching of symbols to numbers using a key. It is likely to measure a variety of cognitive functions including processing speed, associative learning, and working memory (18). As such, the digit-symbol substitution test (DSST) is sensitive to the presence of cognitive dysfunction across a wide range of clinical populations, although it has low specificity for which cognitive domain is affected (18).

Rey auditory-verbal learning test. The Rey auditory-verbal learning test (RAVLT) is a measure of verbal learning and memory (19). Participants are read a noun-word list at a rate of one word per second. They are then asked to recall this list in any order after a delay period—10 min in the present study. Scores range from 0 to 15.

MRI acquisition. Brain MRIs were acquired using 3 Tesla scanners proximal to each CARDIA clinic site. These were Siemens Prisma at Northwestern University, Siemens Tim/Trio at the University of California, Berkley and University of Minnesota, and a Philips Achieva at the University of Alabama, Birmingham. The MRI coordinating center at the University of Pennsylvania collaborated with the MRI field centers to standardize protocols and train technologists. Standardized quality assurance protocols developed for the Functional Bioinformatics Research Network and the Alzheimer's Disease Neuroimaging Initiative were followed by each site to evaluate scanner stability and image distortion (20). T1-weighted (T1w) three-dimensional (3D) magnetization prepared rapid gradient echo images were acquired, and a 4-min T2* resting-state fMRI scan was performed with voxel resolution = 3.5 × 3.5 × 3.5, field of view (FOV) = 224 × 224, matrix = 64 × 64, repetition time

Table 1. Demographic and clinical characteristics of sample (*n* = 578)

Variable	Mean or No.
Age in years (SD)	55 (4)
Sex, male (%)/female (%)	255 (44)/323 (56)
Race, White (%)/Black (%)	335 (58)/243 (42)
Education in years (SD)	15 (3)
Y_{30} Stroop (SD)	22 (11)
Y_{30} CatFluency*	21 (5)
Y_{30} MoCA (SD)†	24 (4)
Y_{30} DSST (SD)‡	69 (17)
Y_{30} RAVLT (SD)§	9 (2)
Y_{30} SBP, mm Hg (SD)	117 (15)
Y_{30} DBP, mm Hg (SD)	72 (11)
Y_{30} BMI (SD)	28 (5)
Y_{30} Cholesterol, mm/dL (SD)	195 (37)
Y_{30} Fasting glucose, mg/dL (SD)	97 (16)
Y_{30} Smoking pack years (SD)	5 (10)
cSBP, mm Hg in 30 y (SD)	3,341 (293)
cDBP, mm Hg in 30 y (SD)	2,113 (234)
Y_{30} raw WMH volume, mm³ (SD)	886 (1,421)
Y_{30} transformed WMH, mm³ (SD)	0.66 (0.42)

BMI = body mass index.
*n = 573.
†n = 575.
‡n = 577.
§n = 576.

(TR) = 2,000, echo time (TE) = 25, and flip = 75. T2-weighted and 3D fluid attenuation inversion recovery (FLAIR) images were also collected along with the T1w images and used to segment WMH.

MRI preprocessing. FSL tools (FMRIB Software Library, https://fsl.fmrib.ox.ac. uk/) were used to preprocess rsfMRI data, including BET (21), with robust brain estimation, FEAT to discard the first 4 s of rsfMRI data, and MCFLIRT motion correction of the functional image. FNIRT applied nonlinear registration between the individuals' structural image and Montreal Neurological Institute (MNI) space with 12 degrees of freedom. ICA-AROMA removed components identified as movement. FAST segmented the T1w image into gray matter, white matter (WM), and cerebrospinal fluid (CSF). Mean time series for WM and CSF were regressed out of the functional data. A high pass filter of 0.01 Hz was applied, and denoised functional data were warped to MNI space. Smoothing was applied using a 6-mm full-width half-maximum kernel.

WMH segmentation. WMH were segmented using an automated machine learning method (22, 23). The support vector machine classifier was first trained using lesions that were manually delineated by expert neuroradiologists. This method then automatically identifies white matter lesions in new scans based on local features extracted from multimodal MRI sequences (i.e., T1-weighted, T2-weighted, and FLAIR).

MRI quality control. Visual inspection of each fMRI scan was performed. Due to the limited field of view for the T2*, many scans were missing brain. A cerebrum mask was used to calculate the percentage of brain missing from each rsfMRI scan. Participants were excluded if they had more than 2% of the total cerebrum missing, or 1% if this involved the dorsal aspect of the brain, which is more important for coregistration. A total of 600 fMRIs were identified as acceptable. In the excluded participants, up to 13% of the cerebrum was missing (mean = 3.4%, SD = 2.2%). Of the remaining 600 individuals who passed quality inspection for rsfMRI, 578 had multiple measures of BP and data for the Stroop task, and these constituted the final sample.

Network estimation using independent components analysis. Preprocessed data from all 600 individuals were entered into a temporally concatenated group independent components analysis (ICA) to generate group-level components using FSL's MELODIC. Automated estimation of model order was used, resulting in 47 independent components (ICs). To objectively determine which ICs reflected functional networks, spatial cross correlation was performed using FSL to identify ICs correlating ≥0.25 with networks previously published by Shirer et al. (24). This cutoff was chosen as it resulted in at least one IC representing each of the 14 Shirer et al. networks (*SI Appendix*, Table S2). More than one IC was allowed to represent a functional network. The left and right executive control networks [LECN and RECN (24)] were considered functional networks relevant to our primary hypothesis for this study. Three executive control ICs, Nos. 11, 13, and 32, were identified (Fig. 2) and examined in relation to Stroop performance using dual regression.

Dual regression to investigate relationship to Stroop performance. For each of the 578 participants with Stroop data, we estimated individual time series and component spatial maps using FSL's dual regression (25). Individual spatial maps for ICs 11, 13, and 32 were merged into four-dimensional files to allow for group-level analysis using randomize nonparametric permutation testing. Voxel-wise nonparametric permutation testing (5,000 permutations) tested for associations with Stroop performance, using threshold-free cluster enhancement (TFCE), which corrects for multiple comparisons across the entire brain. Additional family-wise error (FWE) correction was used to correct for multiple comparisons across the three executive control ICs ($P = 0.05/(2$ tailed $\times 3$ ICs) $= P < 0.008$) based on the TFCE statistic images (26). Covariates included in each model were age, sex, race, education, and site.

Distribution of data. Data were screened for normality prior to statistical analysis. Observations more than three SDs from the mean were Winsorized (27) to the highest value within three SDs of the mean for that variable. For the Stroop, 11 values were Winsorized to the highest value within three SDs of the mean [i.e., 55 (*SI Appendix*, Fig. S1)]. WMH volumes were normalized to the intracranial volume. These ranged from 0.00 to 0.01 mm³; therefore, these were transformed by multiplying by 1,000. WMH data are often not normally distributed; thus, a log transformation is typically used to transform WMH data. However, in our sample, this would have resulted in 70 observations falling more than three SDs below the mean. Therefore, we opted for a square root transformation, which resulted in only 13 observations occurring more than three SDs above the mean, which we then Winsorized to within three SDs from the mean to range from 0.00 to 2.05 mm³. The mean time course of connectivity associated with better Stroop performance (IC32-Stroop connectivity; Fig. 3) had six values Winsorized. Partial correlation and mediation analyses described in the *Results* section report these Winsorized values. All other data were normally distributed.
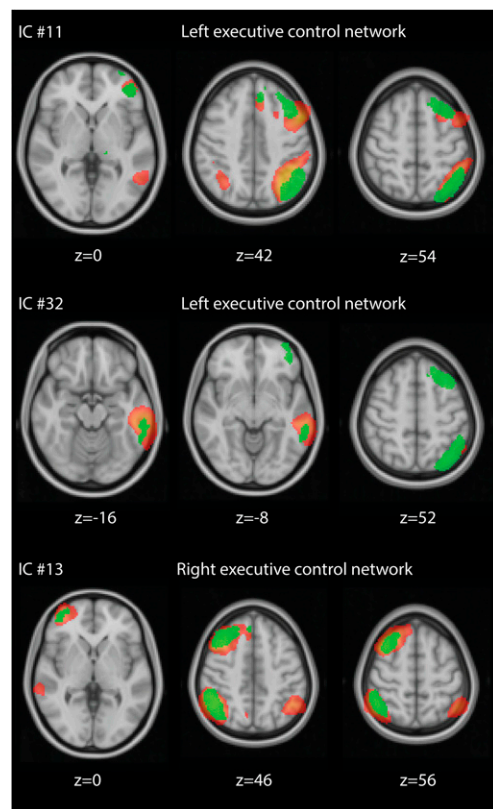
Fig. 2. Three executive control network independent components (red) identified from the group ICA ($n = 600$) and the Shirer et al. components (green).

Testing relationships between Stroop, connectivity, WMH, and cSBP. Simple correlations between cognitive scores, VRFs, and demographic variables are reported in *SI Appendix*, Table S3.

Partial correlations between these variables controlling for age, sex, race, education, and site are reported in *SI Appendix*, Table S4.

To test our mediation hypothesis, we began by conducting a mediation analysis to confirm the previously established mediating effect of WMH on the relationship between BP (cSBP, X) and cognition (Stroop, Y), covarying age, sex, race, and education. PROCESS (version 3.4) was used to perform the analysis (28). To evaluate whether IC32-Stroop connectivity mediated the relationship between WMH and Stroop performance, a mediation analysis was performed with Stroop as the predicted variable (Y) and WMH as the predictor (X). To address concerns related to potential inflated mediation estimates arising from using resting-state connectivity related to Stroop performance (IC32-Stroop connectivity) as a mediator of the relationship between WMH and Stroop performance, we performed additional mediation analyses predicting non-Stroop cognitive performance. This included the CatFluency for an alternate measure of executive function, for which there was data for 573 of the 578 individuals with Stroop data. We also report in the results a mediation analysis with the MoCA to investigate the generalizability of the mediation effect to nonexecutive function measures of cognition. Mediation analyses for the DSST and RAVLT are also reported in *SI Appendix*, Fig. S2. Covariates in all analyses were age, sex, race, education, and site.

Results

The group ICA of 578 participants resulted in 47 ICs. Three ICs spatially correlated with ECNs established by Shirer et al. (24), two with the LECN (IC No. 11 and IC No. 32) and one with the RECN (IC No. 13). ICs are shown in red in Fig. 2, in which green represents the Shirer et al. network masks.

Stroop and Network Connectivity. Results from the dual regression of IC No. 32 are shown in Fig. 3. Green areas are regions in which greater connectivity with IC No. 32 (LECN) is associated
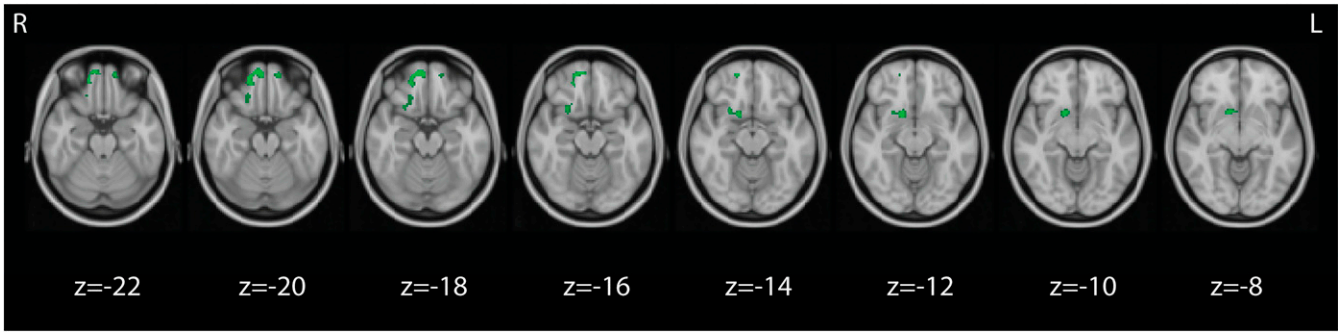
Jenkins et al.
Blood pressure, executive function, and network connectivity in middle-aged adults at risk of dementia in late life

PNAS | 3 of 7
https://doi.org/10.1073/pnas.2024265118

Fig. 3. Regions in green show where greater connectivity with IC No. 32 is associated with better performance on the Stroop. Data are in radiological convention (right = left).

with a better Stroop interference score. These include the bilateral anterior gyrus rectus, right posterior orbitofrontal cortex (OFC), and nucleus accumbens (NAcc). We refer to this as IC32-Stroop connectivity. The results from the dual regression of the other executive control ICs (Nos. 11 and 13) did not survive FWE multiple comparison correction and therefore were not considered further.

The mean time course of IC32-Stroop connectivity (green clusters in Fig. 3) was extracted for each individual for partial correlation and mediation analysis.

BP, Stroop, and Network Connectivity. There was a significant partial correlation between Stroop performance and IC32-Stroop connectivity ($r = -0.251$, $P < 0.001$); however, this significant result was expected, as this connectivity was defined by its association with Stroop performance. Positive partial correlations were also observed between Stroop performance and WMH volume ($r = 0.112$, $P = 0.008$) and between Stroop performance and cSBP ($r = 0.120$, $P = 0.004$). There was also a significant positive partial correlation between WMH and cSBP ($r = 0.130$, $P = 0.002$). There was a significant negative partial correlation between CatFluency, for which higher values indicate better performance, and Stroop performance, for which lower values indicate better performance ($r = -0.183$, $P < 0.001$). Partial correlations also found that CatFluency was significantly negatively correlated with cSBP ($r = -0.153$, $P < 0.001$) but not WMH volume ($r = 0.027$, $P = 0.516$) (*SI Appendix,* Table S4).

The mediation analysis in Fig. 4*A* shows a significant direct effect (c′) of cSBP on Stroop (0.11, SE = 0.04, $P = 0.0107$, 95% CI = 0.03 to 0.19). There was a significant indirect effect of WMH (ab) indicating that WMH significantly mediated the relationship between cSBP and Stroop (ab = 0.01, SE = 0.01, 95% CI = 0.0009 to 0.0330). Next, we evaluated whether IC32-Stroop connectivity mediated the relationship between WMH and Stroop performance. There was a significant direct effect (c′) of WMH on Stroop (0.09, SE = 0.04, $P = 0.0221$, 95% CI = 0.01 to 0.17). Fig. 4*B* shows that IC32-Stroop connectivity mediated this relationship (ab = 0.02, SE = 0.01, 95% CI = 0.01 to 0.05). The observed mediation effect was not specific to Stroop performance. Fig. 4*C* shows that although there was not a direct effect of WMH on the CatFluency (0.03, SE = 0.04, $P = 0.4595$, 95% CI = −0.05 to 0.11), IC32-Stroop connectivity significantly mediated the relationship between WMH and CatFluency (ab = −0.01, SE = 0.01, 95% CI = −0.0211 to −0.0003). Furthermore, Fig. 4*D* shows that although there was not a direct effect of WMH on the MoCA (−0.04, SE = 0.04, $P = 0.2408$, 95% CI = −0.12 to 0.45), IC32-Stroop connectivity significantly mediated the relationship between WMH and MoCA score (ab = −0.01, SE = 0.01, 95% CI = −0.03 to −0.01). Similarly, IC32-Stroop connectivity also mediated the relationship between WMH and DSST performance and between WMH and RAVLT

performance (*SI Appendix,* Fig. S2). *SI Appendix,* Table S5 reports all mediation models in full.

Exploratory analyses investigating cross-network connectivity between higher-level cognitive networks theoretically involved in Stroop performance and networks affected by vascular risk, using
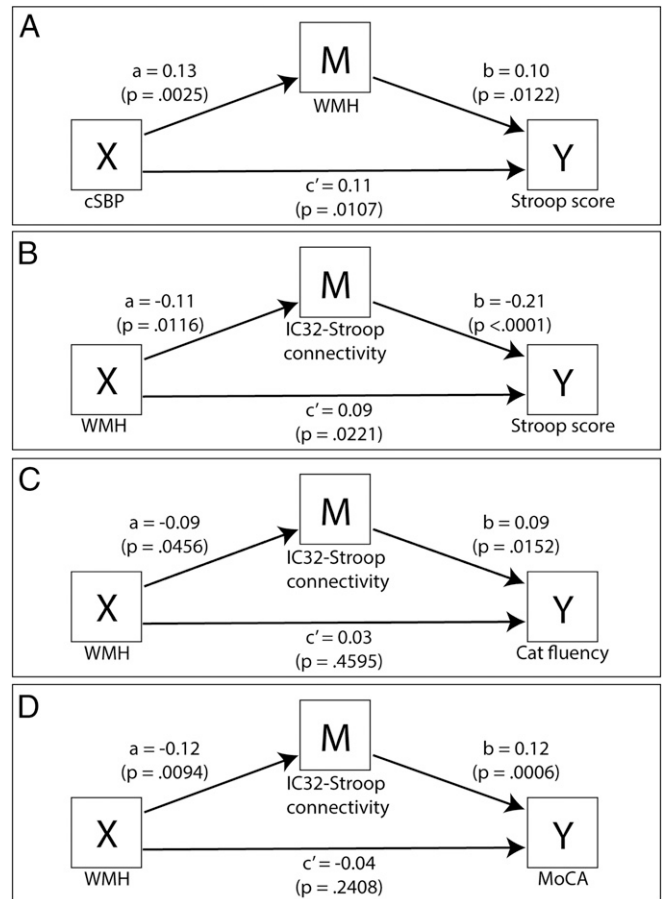

Fig. 4. Results of mediation analyses. *A* confirms the previously established mediating effect of WMH (M) on the relationship between BP (cSBP, X) and cognition (Stroop, Y). *B* shows that the relationship between WMH (X) and Stroop (Y) is significantly mediated by IC32-Stroop connectivity (M). *C* shows that the relationship between WMH (X) and CatFluency (Y) is significantly mediated by IC32-Stroop connectivity (M). *D* shows that the relationship between WMH (X) and MoCA (Y) is also significantly mediated by IC32-Stroop connectivity (M). Note: All mediation models covary age, sex, race, education, and site. cSBP, WMH, IC32-Stroop connectivity values, Stroop score, CatFluency, and MoCA score have been z-transformed to allow effect size comparisons.

FSLNets (29), are reported in *SI Appendix*, Fig. S3 and Tables S6 and S7.

Discussion

The deleterious impact of VRF on brain structure and function and subsequent manifestation of cognitive decline and dementia in late life is well established. How these entities are related in midlife is not known. We examined the relationships between resting-state fMRI network connectivity, executive function, WMH, and cSBP in midlife. We found that greater connectivity of IC No. 32 to regions important for reward processing (the bilateral anterior gyrus rectus, right posterior OFC, and the right NAcc) was associated with better Stroop performance. As hypothesized, we also found that while the previously established relationship of SBP to Stroop performance was mediated by WMH, IC32-Stroop connectivity mediated the relationship between WMH and Stroop. Additional analyses found that this IC32-Stroop connectivity mediated the relationship between WMH and performance on another measure of executive function, the CatFluency test. Furthermore, the mediation effect generalized to a more general measure of cognition, the MoCA, indicating that the effect was not specific to the Stroop task. Mechanistically, our findings suggest that higher cumulative BP exposure during young adulthood is related to worse executive function and broad cognitive performance in midlife, mediated via WMH, especially in those individuals with lower connectivity of IC No. 32 to regions important for reward processing. Hence, functional network connectivity could provide a compensatory mechanism to preserve cognitive performance in the context of WMH and small-vessel disease.

The relationship between WMH and impaired cognition, in particular executive function, is well established (30–33). In the present study, partial correlations also replicated prior findings linking WMH volumes with Stroop performance (12, 13). A disconnection state has been posited as the underlying mechanism linking WM integrity and cognitive decline (31). Yet there are considerable individual differences in the relationship between WMH and cognition (34, 35). Adequate cognitive performance in the presence of high amounts of neuropathology, such as WMH, has been explained using the concept of cognitive reserve, whereby the brain utilizes strategies to compensate for pathology (34, 36), including the recruitment of cognitive processes and neural networks (37, 38). Frontoparietal connectivity has particularly been reported to have a protective role and be a potential neural substrate for cognitive reserve in normal and pathological aging (39). Similarly, we found that better Stroop performance was associated with greater connectivity between an IC that was spatially correlated with the LECN and the OFC and NAcc. These regions are part of the emotion and salience network and are crucial for reward processing, including encoding novel information (40) (necessary for reward learning), representing the reward value of stimuli (41), and guiding reward-related behavior (42). Reduced regulation of reward regions by the ECN is characteristic of impaired behavioral control, including in individuals with pathological gambling, internet gaming disorder, impaired control of food consumption, and with substance addictions (e.g., heroin and nicotine) (43). Therefore, it is not surprising that better performance on the Stroop task was associated with increased connectivity of an LECN IC and reward-processing regions.

While we were primarily interested in the relationship between cSBP, WMH, resting-state connectivity, and Stroop performance, we also examined cDBP in relation to these variables. Simple (*SI Appendix*, Table S3) and most partial correlation analyses (*SI Appendix*, Table S4) showed similar but slightly weaker relationships between cDBP and cognitive variables than cSBP. A mediation analysis found that although there was no direct relationship between cDBP and Stroop (when accounting for covariates), WMH did mediate this relationship (*SI Appendix*, Fig. S2 and Table S5, Section B). Importantly, we also examined

measures of executive function and cognition other than the Stroop, and found that IC32-Stroop connectivity also mediated the relationship between WMH and performance on the CatFluency, MoCA, DSST, and RAVLT. Low scores on these measures have also been associated with cardiovascular health, both within the broader CARDIA sample (44) and in independent studies (45, 46), including an association with increased risk of 5-y mortality in a large cardiovascular health study (47). Our finding that IC32-Stroop connectivity mediates the relationship between WMH and scores on these additional measures is further evidence that this connectivity is reflective of cognitive reserve.

Our findings are consistent with Ye et al. (35), who studied adults with a similar age to our sample. They also found that individuals with WMH and cognitive impairment (but not those without cognitive impairment) had increased functional connectivity of the left superior parietal gyrus with frontal regions, which was associated with less executive dysfunction. Our results also support those of Benson et al. (48), who found that in nondemented individuals aged 50 to 80, greater connectivity of frontoparietal nodes moderated the relationship between WMH and executive function. Whereas Benson et al. found a moderation effect and we found a mediation effect, both studies show that the negative impact of WMH on executive functions was either reduced or eliminated in individuals with higher levels of resting-state connectivity of cognitive control networks. Further, Benson et al. found their moderation effect using seed-to-seed connectivity of frontoparietal nodes to each other, whereas we found our mediation effect using a data-driven analysis of connectivity of an IC correlated with the LECN to regions of the reward and salience network. However, also consistent with our study was the finding by Benson et al. that salience network connectivity associated with cognitive reserve moderated the relationship between WMH and executive function. Benson et al. concluded that their results were consistent with the conception that higher functional connectivity in ECNs may serve as a protective neural mechanism, allowing better preservation of cognitive ability when cerebrovascular pathology is present. Other researchers who have also reported associations between WMH volume and functional connectivity have interpreted these findings as reflecting compensatory or neuroplastic reorganization of functional connectivity following disruption to WM tracts even in the absence of overt disease (33, 49). We argue that our results also support these conclusions and further extend this literature by demonstrating the link to cumulative BP exposure.

The contribution of structural loss to aberrant functional connectivity is important to understand. VRFs are associated with reduced WM integrity as well as reduced cerebral gray matter integrity. For example, we have demonstrated previously in a subset of the present sample that cSBP is related to morphology of the basal ganglia and thalamus (8). More recently, Veldsman et al. (50), in a cross-sectional study, examined the role of frontoparietal network structure in the relationship between age, VRF, WMH, and executive function in a sample of 22,059 participants from the UK Biobank aged 44 to 73 (mean age: 62; SD: 7). In this very large sample that is older than that of the current study, Veldsman et al. used structural imaging to look at WMH, WM integrity in the superior longitudinal fasciculus (measured with neurite orientation dispersion and density imaging [NODDI]), and gray matter volume of the frontoparietal cortex (defined a priori). Veldsman et al. nicely showed that cerebrovascular risk was associated with reduced cerebral gray and WM integrity within frontoparietal brain structures. They also used mediation analysis to show that the relationship between the predefined frontoparietal gray matter volumes and executive function was mediated through the integrity of the predefined frontoparietal white matter (superior longitudinal fasciculus) as measured by NODDI. Their structural data provide support for the proposed cortical "disconnection" as a mechanism of age-related cognitive decline.

Jenkins et al.
Blood pressure, executive function, and network connectivity in middle-aged adults at risk of dementia in late life

PNAS | 5 of 7
https://doi.org/10.1073/pnas.2024265118
www.manaraa.com

Another important mechanistic hypothesis in vascular brain aging relates to the concept of cognitive reserve. A number of studies have shown that protective lifestyle factors attenuate cognitive dysfunction related to WMH. This mechanism has been best supported not by structural neuroimaging studies but rather by functional neuroimaging studies such as this one and those described previously (e.g., ref. 48) that suggest that higher cognitive reserve may be associated with brain activation patterns that reflect greater neural connectivity. Our study is specifically designed to explore such early pathways and mechanisms in a unique community-based population; that is, a midlife population with repeated measures of BP collected across early adult life to midlife that allows us to explore a quantitative effect of BP exposure rather than the simple presence or absence of hypertension or BP-lowering treatment. This is a significant area of knowledge gap and is mechanistically important to explore before multiple age-related comorbidities set in and disentangling pathways becomes difficult. So, with a focus on cognitive reserve, we present confirmatory evidence for our hypotheses that 1) greater rsfMRI functional connectivity of ECNs would be related to better performance in an executive control task and 2) while the previously established relationship of SBP to executive performance would be mediated by WMH (a measure of brain vascular exposure and small vessel disease), the established relationship between WMH and executive performance would be mediated by ECN connectivity.

Limitations. Our study has several limitations. To begin with, only 4 min of resting-state data were collected, which is likely to increase the noise in our data and reduce the power to detect significant results. However, other similar studies have reported similarly brief resting-state protocols [e.g., 5 min and 25 s (33) and 6 min (9)] but with much smaller samples. Additional noise in our dataset likely came from the fact that participants were not instructed to keep their eyes open or closed during resting-state fMRI. Another limitation was that FOV restrictions in the rsfMRI protocol resulted in the exclusion of a large number of participants from our sample. Only supratentorial regions were examined; however, we note that a similar study did not examine the cerebellum (9). It would be important to determine to what extent the compensatory effect of the connectivity of IC32-Stroop is due to reduced structural integrity of this ECN. Structural integrity influencing intrinsic network connectivity includes both gray and WM. In addition, both are affected by VRF. Therefore, to determine the nature of independent contributions to functional connectivity, a careful delineation of both gray matter as well as WM in this region would be necessary; however, that is beyond the scope of the present study. Also, our midlife sample was relatively healthy, and, as such, age-related gray and WM loss and atrophy may not be as prominent as that seen in the older cohorts in prior studies. In support of this statement, in a subsample of the present study, we previously found no significant correlations between volume of the basal ganglia and thalamus and cSBP or DBP, but we did find that WMH were significantly correlated with both cSBP and cDBP (8). So, while not covarying for gray (cortical) and WM atrophy remains a limitation of our study, it is not unreasonable to assume that the impact of these variables in this midlife, relatively healthy cohort would be less than that seen in some of the more aged cohorts we discussed. As such, the extent to which our results apply to older individuals and those with a higher burden of vascular risk factors remains to be determined in future studies.

Furthermore, at least one study in older adults without cognitive impairment has shown that the relationship between WMH and cognition is independent of atrophy (51). The sample of the present study had a relatively high mean and median level of education (16), with only 24 participants reporting less than a high-school education. As such, it is unclear to what extent the present results are generalizable to individuals with less education. The longitudinal BP measurements collected at nine time points were a strength of the study; however, levels of BP control in between visits are unknown, potentially confounding results. Finally, there were significant between-site differences in VRF and demographic variables, which required statistical covariation. While not ideal, the large range of these values in our dataset may enhance the generalizability of our results. Together, these limitations are likely to have affected the quality of our results. Undoubtedly, the large sample size of this study increased the power to detect significant findings.

Conclusions

Using rsfMRI in a large midlife sample of adults with well-characterized VRF, we identified regions of functional connectivity to the LECN that may compensate for impaired executive control performance in the context of WMH and small-vessel disease. Our results are consistent with previous findings that show the importance of cognitive control and salience network connectivity for reserve in the context of cerebrovascular pathology (48). In the future, compensatory brain regions or networks involved in cognitive reserve could be potential targets for therapeutic intervention to preserve brain health and cognitive function. For example, repetitive transcranial magnetic stimulation has been associated with improved performance on the Stroop in young, healthy individuals (52), normal aging (53), and patients with cerebrovascular disease (54). Longitudinal follow-up studies in samples such as CARDIA will be able to track network connectivity in the context of increasing BP exposure and cerebrovascular pathology burden to examine the influence of vascular disease on cognitive and rsfMRI functional connectivity changes over time.

Our results support the position that neuroplastic reorganization of functional connectivity occurs with disruptions in WM tracts even in the absence of overt disease (33, 49), as was the burden of cerebrovascular pathology in our midlife sample. Connectivity in these resting-state functional networks may be one compensatory mechanism to preserve executive function in individuals with VRF and WMH.

1. R. F. Gottesman et al., Midlife hypertension and 20-year cognitive change: The atherosclerosis risk in communities neurocognitive study. JAMA Neurol. 71, 1218–1227 (2014).
2. L. J. Launer, K. Masaki, H. Petrovitch, D. Foley, R. J. Havlik, The association between midlife blood pressure levels and late-life cognitive function. The Honolulu-Asia Aging Study. JAMA 274, 1846–1851 (1995).
3. G. E. Swan, D. Carmelli, A. Larue, Systolic blood pressure tracking over 25 to 30 years and cognitive performance in older adults. Stroke 29, 2334–2340 (1998).
4. G. E. Swan et al., Association of midlife blood pressure to late-life cognitive decline and brain morphology. Neurology 51, 986–993 (1998).
5. American Psychiatric Association, Diagnostic and Statistical Manual of Mental Disorders (American Psychiatric Association, Washington, DC, ed. 5, 2013).
6. T. Jeerakathil et al., Stroke risk profile predicts white matter hyperintensity volume: The Framingham Study. Stroke 35, 1857–1861 (2004).
7. O. Beauchet et al., Blood pressure levels and brain volume reduction: A systematic review and meta-analysis. J. Hypertens. 31, 1502–1516 (2013).

6 of 7 | PNAS
https://doi.org/10.1073/pnas.2024265118

Jenkins et al.
Blood pressure, executive function, and network connectivity in middle-aged adults at risk

8. L. M. Jenkins *et al.*, Cumulative blood pressure exposure, basal ganglia, and thalamic morphology in midlife. *Hypertension* **75**, 1289–1295 (2020).

9. J. M. Spielberg *et al.*, Higher serum cholesterol is associated with intensified age-related neural network decoupling and cognitive decline in early- to mid-life. *Hum. Brain Mapp.* **38**, 3249–3261 (2017).

10. F. Beyer *et al.*, Higher body mass index is associated with reduced posterior default mode connectivity in older adults. *Hum. Brain Mapp.* **38**, 3502–3515 (2017).

11. C. Spinelli *et al.*, Impaired cognitive executive dysfunction in adult treated hypertensives with a confirmed diagnosis of poorly controlled blood pressure. *Int. J. Med. Sci.* **11**, 771–778 (2014).

12. J. H. Kim *et al.*, Regional white matter hyperintensities in normal aging, single domain amnestic mild cognitive impairment, and mild Alzheimer's disease. *J. Clin. Neurosci.* **18**, 1101–1106 (2011).

13. J. H. Kramer, B. R. Reed, D. Mungas, M. W. Weiner, H. C. Chui, Executive dysfunction in subcortical ischaemic vascular disease. *J. Neurol. Neurosurg. Psychiatry* **72**, 217–220 (2002).

14. Y. Yano *et al.*, Long-term blood pressure variability throughout young adulthood and cognitive function in midlife: The Coronary Artery Risk Development in Young Adults (CARDIA) Study. *Hypertension* **64**, 983 (2014).

15. Y. Yano *et al.*, Visit-to-visit blood pressure variability in young adulthood and hippocampal volume and integrity at middle age: The CARDIA study (Coronary Artery Risk Development in Young Adults). *Hypertension* **70**, 1091–1098 (2017).

16. M. B. Jurado, M. Rosselli, The elusive nature of executive functions: A review of our current understanding. *Neuropsychol. Rev.* **17**, 213–233 (2007).

17. Z. S. Nasreddine *et al.*, The Montreal Cognitive Assessment, MoCA: A brief screening tool for mild cognitive impairment. *J. Am. Geriatr. Soc.* **53**, 695–699 (2005).

18. J. Jaeger, Digit Symbol Substitution Test: The case for sensitivity over specificity in neuropsychological testing. *J. Clin. Psychopharmacol.* **38**, 513–519 (2018).

19. D. Bowler, "Rey Auditory Verbal Learning Test (Rey AVLT)" in *Encyclopedia of Autism Spectrum Disorders*, F. R. Volkmar, Ed. (Springer, New York, NY, 2013).

20. L. J. Launer *et al.*, Vascular factors and multiple measures of early brain health: CARDIA brain MRI study. *PLoS One* **10**, e0122138 (2015).

21. S. M. Smith, Fast robust automated brain extraction. *Hum. Brain Mapp.* **17**, 143–155 (2002).

22. Z. Lao *et al.*, Computer-assisted segmentation of white matter lesions in 3D MR images using support vector machine. *Acad. Radiol.* **15**, 300–313 (2008).

23. E. I. Zacharaki, S. Kanterakis, R. N. Bryan, C. Davatzikos, Measuring brain lesion progression with a supervised tissue classification system. *Med. Image Comput. Comput. Assist. Interv.* **11**, 620–627 (2008).

24. W. R. Shirer, S. Ryali, E. Rykhlevskaia, V. Menon, M. D. Greicius, Decoding subject-driven cognitive states with whole-brain connectivity patterns. *Cereb. Cortex* **22**, 158–165 (2012).

25. L. D. Nickerson, S. M. Smith, D. Öngür, C. F. Beckmann, Using dual regression to investigate network shape and amplitude in functional connectivity analysis. *Front. Neurosci.* **11**, 115 (2017).

26. S. M. Smith, T. E. Nichols, Threshold-free cluster enhancement: Addressing problems of smoothing, threshold dependence and localisation in cluster inference. *Neuroimage* **44**, 83–98 (2009).

27. W. J. Dixon, Simplified estimation from censored normal samples. *Ann. Math. Stat.* **31**, 385–391 (1960).

28. A. F. Hayes, *Introduction to Mediation, Moderation and Conditional Process Analysis: A Regression-Based Approach* (Guilford Press, New York, ed. 2, 2018).

29. S. M. Smith *et al.*, Functional connectomics from resting-state fMRI. *Trends Cogn. Sci.* **17**, 666–682 (2013).

30. F. M. Gunning-Dixon, N. Raz, Neuroanatomical correlates of selected executive functions in middle-aged and older adults: A prospective MRI study. *Neuropsychologia* **41**, 1929–1941 (2003).

31. F. M. Gunning-Dixon, A. M. Brickman, J. C. Cheng, G. S. Alexopoulos, Aging of cerebral white matter: A review of MRI findings. *Int. J. Geriatr. Psychiatry* **24**, 109–117 (2009).

32. M. Tullberg *et al.*, White matter lesions impair frontal lobe function regardless of their location. *Neurology* **63**, 246–253 (2004).

33. M. De Marco, R. Manca, M. Mitolo, A. Venneri, White matter hyperintensity load modulates brain morphometry and brain connectivity in healthy adults: A neuroplastic mechanism? *Neural Plast.* **2017**, 4050536 (2017).

34. A. M. Brickman *et al.*, White matter hyperintensities and cognition: Testing the reserve hypothesis. *Neurobiol. Aging* **32**, 1588–1598 (2011).

35. Q. Ye *et al.*, Enhanced regional homogeneity and functional connectivity in subjects with white matter hyperintensities and cognitive impairment. *Front. Neurosci.* **13**, 695 (2019).

36. Y. Stern, Cognitive reserve. *Neuropsychologia* **47**, 2015–2028 (2009).

37. D. Bartrés-Faz, E. M. Arenaza-Urquijo, Structural and functional imaging correlates of cognitive and brain reserve hypotheses in healthy and pathological aging. *Brain Topogr.* **24**, 340–357 (2011).

38. P. A. Reuter-Lorenz, D. C. Park, How does it STAC up? Revisiting the scaffolding theory of aging and cognition. *Neuropsychol. Rev.* **24**, 355–370 (2014).

39. N. Franzmeier *et al.*, Left frontal hub connectivity during memory performance supports reserve in aging and mild cognitive impairment. *J. Alzheimers Dis.* **59**, 1381–1392 (2017).

40. S. Frey, M. Petrides, Orbitofrontal cortex: A key prefrontal region for encoding information. *Proc. Natl. Acad. Sci. U.S.A.* **97**, 8723–8727 (2000).

41. M. L. Kringelbach, E. T. Rolls, The functional neuroanatomy of the human orbitofrontal cortex: Evidence from neuroimaging and neuropsychology. *Prog. Neurobiol.* **72**, 341–372 (2004).

42. D. Öngür, J. L. Price, The organization of networks within the orbital and medial prefrontal cortex of rats, monkeys and humans. *Cereb. Cortex* **10**, 206–219 (2000).

43. R. Z. Goldstein, N. D. Volkow, Dysfunction of the prefrontal cortex in addiction: Neuroimaging findings and clinical implications. *Nat. Rev. Neurosci.* **12**, 652–669 (2011).

44. J. P. Reis *et al.*, Cardiovascular health through young adulthood and cognitive functioning in midlife. *Ann. Neurol.* **73**, 170–179 (2013).

45. A. Noriega de la Colina *et al.*, Diurnal blood pressure loads are associated with lower cognitive performances in controlled-hypertensive elderly individuals. *J. Hypertens.* **37**, 2168–2179 (2019).

46. R. A. H. Stewart *et al.*, Cardiovascular and lifestyle risk factors and cognitive function in patients with stable coronary heart disease. *J. Am. Heart Assoc.* **8**, e010641 (2019).

47. L. P. Fried *et al.*, Risk factors for 5-year mortality in older adults: The Cardiovascular Health Study. *JAMA* **279**, 585–592 (1998).

48. G. Benson *et al.*, Functional connectivity in cognitive control networks mitigates the impact of white matter lesions in the elderly. *Alzheimers Res. Ther.* **10**, 109 (2018).

49. Y. D. Reijmer *et al.*, Decoupling of structural and functional brain connectivity in older adults with white matter hyperintensities. *Neuroimage* **117**, 222–229 (2015).

50. M. Veldsman *et al.*, Cerebrovascular risk factors impact frontoparietal network integrity and executive function in healthy ageing. *Nat. Commun.* **11**, 4340 (2020).

51. Z. Arvanitakis *et al.*, Association of white matter hyperintensities and gray matter volume with cognition in older individuals without cognitive impairment. *Brain Struct. Funct.* **221**, 2135–2146 (2016).

52. Y. Li *et al.*, The effects of high-frequency rTMS over the left DLPFC on cognitive control in young healthy participants. *PLoS One* **12**, e0179430 (2017).

53. S. H. Kim, H. J. Han, H. M. Ahn, S. A. Kim, S. E. Kim, Effects of five daily high-frequency rTMS on Stroop task performance in aging individuals. *Neurosci. Res.* **74**, 256–260 (2012).

54. I. Rektorova, S. Megova, M. Bares, I. Rektor, Cognitive functioning after repetitive transcranial magnetic stimulation in patients with cerebrovascular disease without dementia: A pilot study of seven patients. *J. Neurol. Sci.* **229–230**, 157–161 (2005).

Jenkins et al.
Blood pressure, executive function, and network connectivity in middle-aged adults at risk of dementia in late life

PNAS | 7 of 7
https://doi.org/10.1073/pnas.2024265118

www.manaraa.com